Quantum Electronics **50** (3) 309–314 (2020)

https://doi.org/10.1070/QEL17124

Temperature estimation in a spatially inhomogeneous flame by diode laser absorption spectroscopy

V.V. Liger, V.R. Mironenko, Yu.A. Kuritsyn, M.A. Bolshov

Abstract. **A two-temperature (2*T*) model is proposed for estimating the temperature of a spatially inhomogeneous hot zone using single-beam diode laser absorption spectrometry. The proposed algorithm is based on fitting experimental absorption spectra by a linear combination of two database-simulated single-temperature spectra with different temperatures. The model efficiency is experimentally demonstrated when determining the temperature in different flame zones of a Wolfgard–Parker slot burner. The proposed 2*T* algorithm is used to find the maximum and minimum temperatures in different flame sections, which are compared with local temperatures in the same flame zones measured by the method of coherent anti-Stokes Raman scattering (CARS). It is shown that the maximum temperatures determined by the proposed 2*T* algorithm are in good agreement with CARS data in flame zones where high-temperature regions prevail. A good agreement between the minimum temperatures obtained by these two methods is also observed for predominantly cold zones.**

Keywords: *absorption spectroscopy, diode laser, temperature measurement.*

1. Introduction

Optical sensors based on tunable diode laser absorption spectroscopy (DLAS) are widely used for contactless diagnostics of parameters of various hot zones [1–6]. The main advantages of DLAS sensors are a relatively simple design, a comparatively low cost of their components, as well as the ability to place sensitive parts of the sensor away from the test object and deliver probe laser radiation to the test object via optical fibre.

To date, various sensor designs have been developed for detecting the main molecular components of the hot zone. As a rule, sensors are based on recording the absorption spectra of the selected molecule. Typical molecules can be water molecules, carbon oxides, various hydrocarbons, i.e. molecules that are the main components of the combustion process. The main parameter of the hot zone, i.e. temperature, is determined either by the ratio of the integral absorption intensities or by fitting experimental spectra by theoretical ones, simulated using spectroscopic databases.

V.V. Liger, V.R. Mironenko, Yu.A. Kuritsyn, M.A. Bolshov Institute for Spectroscopy, Russian Academy of Sciences, ul. Fizicheskaya 5, Troitsk, 108840 Moscow, Russia;
e-mail: mbolshov@mail.ru; bolshov@isan.troitsk.ru

Received 3 September 2019; revision received 11 December 2019
Kvantovaya Elektronika **50** (3) 309–314 (2020)
Translated by M.A. Monastyrskiy

When implementing the simplest scenario of DLAS, the probe laser beam is transmitted through the object under study, and the transmitted radiation spectrum is recorded. This scenario, when the absorption spectrum is formed along the entire path of the beam from the source to the receiver, is called trace probing. The problem of diagnosing a spatially inhomogeneous hot zone in which the temperature and concentration of absorbing molecules change along the trace arises during the trace probing. In this case, the radiation absorption changes not only within the probed object, but also on the beam path outside the object. Due to this, the spectrum formed on the entire trace is a superposition of the spectra formed on individual sections of the trace, while there may be sections on the trace with a relatively uniform distribution of temperature and concentration, as well as with strong gradients of these parameters.

In our previous works containing the results of trace probing of hot objects, this circumstance has not been taken into account, and the temperature was determined by fitting the experimental spectrum to the theoretical one simulated using the HITRAN and HITEMP databases [7, 8] with the same temperature and pressure. Obviously, this algorithm (for short, we call it the 1*T* algorithm) gives a certain temperature which is lower than the maximum temperature T_{max} of the object, but greater than its minimum temperature T_{min}. Hereafter, we call the temperature of an inhomogeneous medium, determined using the 1*T* processing algorithm, the effective temperature T_{eff}.

The most radical way to solve the problem of inhomogeneity of medium parameters is to use the tomographic approach, in which the laser beam is split into a set of beams that intersect the volume under study in perpendicular directions [9–11]. However, this approach significantly complicates the DLAS sensor design and the processing algorithm, as well as increases the sensor cost. An even more serious limitation of the tomographic approach is the inability to probe closed volumes inside internal combustion chambers or power units. Tomography gives good results when probing open areas of such emissions of exhaust combustible gases into the atmosphere.

In work [12], we proposed a new algorithm for processing experimental absorption spectra to determine the maximum temperature of the inhomogeneous combustion zone, in which the experimental spectrum of radiation that passed through the inhomogeneous zone was fitted by a linear combination of two single-temperature spectra with the corresponding weights of each spectrum. These weights, along with other parameters, are fitting parameters. This processing algorithm is further called the 2*T* algorithm. In work [12], experiments were performed using two cells with different

temperatures, located in the path of the laser beam. A good agreement between the temperatures determined by the trace DLAS using the $2T$ processing algorithm and the temperatures measured by thermocouples confirmed the effectiveness of the proposed algorithm.

The aim of this work was to verify the operability of the proposed algorithm when determining the temperature in various zones of the slit burner flame, which is an example of a spatially inhomogeneous hot zone. The flame was probed using the DLAS method, while its maximum and minimum temperatures were determined using the $2T$ algorithm proposed in [12]. The results obtained were compared with the results of measuring local temperatures in the same flame by the method of coherent anti-Stokes Raman scattering (CARS) [13].

2. Theoretical basis

Under conditions of a thermodynamic equilibrium, the temperature is determined by the ratio of the integral intensities of two absorption lines of the molecule with different lower levels of the corresponding transitions. At low absorption, when the linear approximation of the Lambert – Beer law is valid, the measured absorption signal Y_v at the frequency v can be expressed as

$$Y_v = \sum_j S_j(T) g_{jv} NL + b_v + \varepsilon_v = Z_v + b_v + \varepsilon_v, \qquad (1)$$

where $S_j(T)$ is the integral intensity of the line j; g_{jv} is the line profile; N is the concentration of absorbing molecules; L is the absorbing layer length; Z_v is the theoretical spectrum simulated on the basis of spectroscopic databases; b_v is the baseline; and ε_v is the residual (the difference between the experimental and simulated spectra). The integral line intensities are determined during the fitting process which includes the residual minimisation. Expression (1) is valid for a spatially homogeneous medium with a constant temperature along the entire probe trace.

For an inhomogeneous medium, expression (1) does not hold. We proposed to represent an inhomogeneous medium as a superposition of the 'cold' part with the temperature T_{low} and the 'hot' part with the temperature T_{hot} [12]. Then the theoretical spectrum Z_v can be expressed as a linear combination of two spectra depending on two different temperatures, T_{low} and T_{hot}:

$$Z_v = B_1 D_v(T_{low}) + B_2 D_v(T_{hot}), \qquad (2)$$

where $D_v(T_{low})$ and $D_v(T_{hot})$ are the single-temperature spectra for temperatures T_{low} and T_{hot}, respectively; and $B_{1,2}$ are coefficients accounting for the contributions of the cold and hot parts to the resulting spectrum.

In our work [14], we used a prototype of a DLAS spectrometer with two diode lasers operating in different spectral ranges. This version of the spectrometer was chosen because of a significant overlap of the absorption lines at the atmospheric pressure and the temperature of the hot flame zones over 2000 K. Under conditions of significant overlap of the lines, the fitting algorithm included the following steps:

1. A set of absorption lines in each spectral range was selected and used for fitting. The criterion for selecting lines was their intensity, i.e. only lines with an intensity of at least 10^{-2} of the maximum line intensity in the range were taken into account. This criterion was met by 13 H_2O lines in the frequency range 7183.8 – 7186.8 cm^{-1} and 14 lines in the range 7443 – 7446 cm^{-1}.

2. When simulating spectral sections in each range, the positions of the line maxima were taken from the HITRAN database.

3. A linear combination of simulated single-temperature spectra $D_v(T_{low})$ and $D_v(T_{hot})$ was fitted to the experimental spectrum by varying the temperatures T_{low} and T_{hot}, Lorentzian parts of the line profiles and the coefficients B_1 and B_2. When fitting, a 'seed' (initial) partial water vapour pressure of 0.1 atm was selected, while the lengths of the absorbing layers were assumed to be 4 cm. These parameters are close to the parameters of a real experiment.

The temperatures T_{low} and T_{hot} were determined during the fitting process using the nonlinear least squares (NLS) method. In this case, the sum of squared residuals ε_v^2 was minimised:

$$\sum_v \varepsilon_v^2 = \sum_v (Y_v - Z_v - b_v)^2 \to \min. \qquad (3)$$

We have shown that our algorithm is mathematically identical to the correlation algorithm used in work [12]. The application of the NLS method in this paper is explained by the fact that, in contrast to [12], we were not able to create our own experimental database of single-temperature spectra. In hot flame zones, the temperature exceeded 2000 K, while the cells used in [12] withstood a temperature no higher than 1200 K. Therefore, the fitting of the simulated Z_v spectra was performed by means of the NLS method using the HITRAN and HITEMP databases for single-temperature spectrum simulation.

3. Experimental part

3.1. Flame

As an example of a spatially inhomogeneous hot zone, the laminar flame of the Wolfhard – Parker slot burner was chosen [15, 16]. This burner is compact and, most importantly, its flame parameters, at fixed flow rates of methane and air, are well reproducible during repeated launches. The flame has a planar structure with zones of sufficiently uniform temperature and transition zones from the inner layers to the outer ones with large temperature gradients. The flame parameters can be reproducibly changed by varying the fuel and air consumption. Burners of this design are widely used to test the efficiency of various spectroscopic diagnostic methods.

An enriched mixture of methane with air was used in the work. Electronic sensors ensured the accuracy of establishing the flow rates of fuel and air of 0.01 and 0.1 norm L min^{-1}, respectively, which made it possible to achieve high reproducibility of the flame structure and temperature distribution from start to start.

A detailed description of the structure of the hot zone of the Wolfhard – Parker burner is given in [13]. A schematic of the burner with characteristic dimensions to provide partial preliminary mixing of fuel and oxidiser is shown in Fig. 1a. The flows of homogenised gas arrive separately through three slit channels of rectangular cross section. Mixed fuel (methane) and oxidiser (air) are fed into the central channel with a width of 9 mm, and an additional amount of air enters the side channels and forms a concurrent flow around the flame to stabilise it. In this way, a quasi-stationary flow of heated

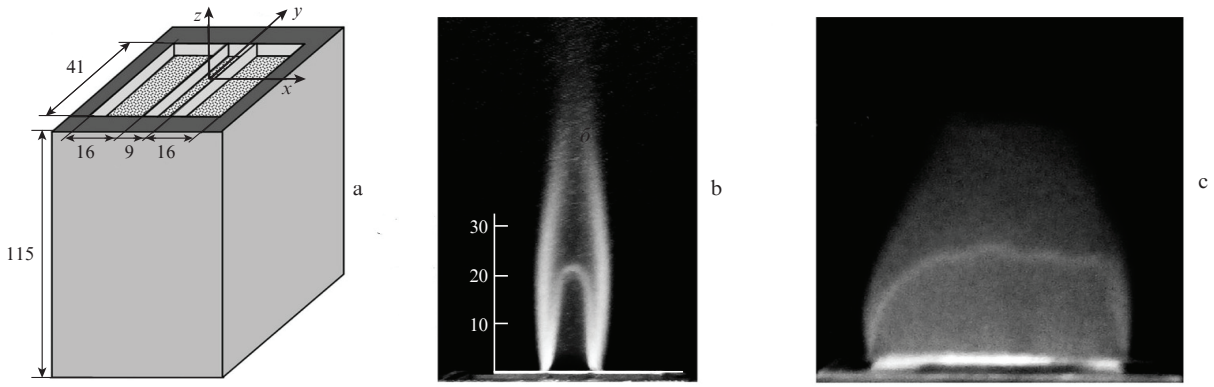

Figure 1. (a) Scheme of a Wolfhard–Parker burner and (b, c) photographs of the flame in (b) *xz* and (c) *yz* planes. All dimensions are given in millimetres.

gas is formed. The burner design assumes the flame symmetry relative to the *yz* plane, close-to-uniform temperature distribution inside the flame along the burner slot (along the *y* axis) and high temperature gradients when passing through the flame front to the outer layers. The burner is mounted on a movable translation stage allowing its housing to be positioned with an accuracy of 0.01 mm along the *x* axis, 0.25 mm along the *z* axis, and 1 mm along the *y* axis.

Photographs of the flame during the combustion of an enriched methane–air mixture with a fuel excess coefficient $\Phi = 2$ are shown in Figs 1b and 1c. The flame symmetry relative to the *yz* plane, as well as the internal and external boundaries of flame fronts are clearly visible. In particular, the inner front height is ~20 mm.

3.2. DLAS spectrometer design

The DLAS spectrometer with two diode lasers was described in detail in [17]. Here we only consider the main components of the spectrometer and the features of its operation. The spectrometer, the scheme of which is shown in Fig. 2, consists of a unit of diode lasers (UDLs), a control and optical signal recording unit (COSRU), a photodetector unit (PU), and a system of optical and electrical cables. In the experiments, we used two distributed feedback diode lasers (DLs) (Sacher Lasertechnik [18]) generating in the spectral ranges 7183.8–7186.8 cm^{-1} ($\lambda \approx 1.39$ μm) and 7443.0–7446.0 cm^{-1} ($\lambda \approx 1.34$ μm). The choice of these DLs is stipulated by the technical specifications for measuring the temperatures of hot zones in the range of 500–2500 K [17].

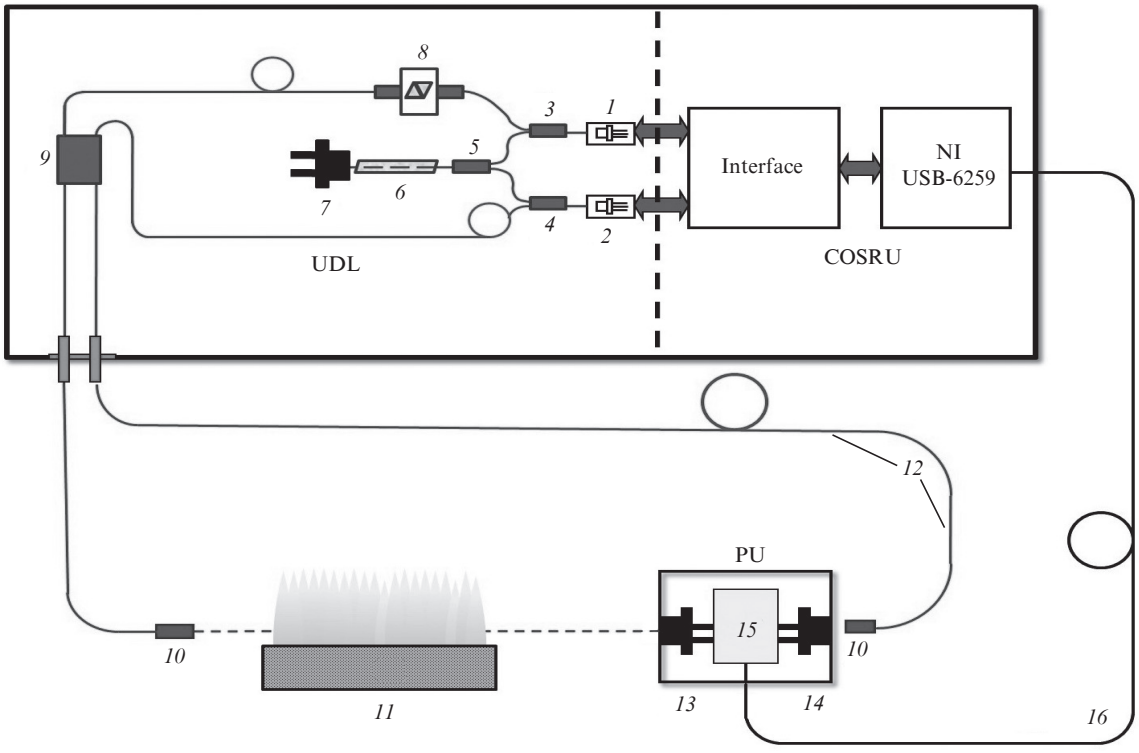

Figure 2. Schematic of the experimental setup: (*1*, *2*) diode lasers; (*3*–*5*, *9*) fibre-optic multiplexers; (*6*) reference cell with water vapour; (*7*) channel-stabilisation photodiode; (*8*) fibre-optic attenuator; (*10*) gradient collimators; (*11*) burner; (*12*) fibre-optic cables; (*13*) measuring channel photodiode; (*14*) reference channel photodiode; (*15*) differential preamplifier; (*16*) electric cable.

The radiation from both DLs is collected in an optical multiplexer (*9*) and introduced into a single-mode fibre. A gradient collimator mounted at the fibre end forms an output beam with low divergence and a diameter of ~1 mm and directs the beam into the flame. The transmitted radiation is collected by the optical system on photodiode *13*. Photodiode *14* measures the output power of both DLs for normalisation when processing absorption signals. This normalisation is necessary to account for changes in the DL radiation intensity when its wavelength is rapidly tuned. The output signals from the photodiodes (*13* and *14*) are sent to a differential preamplifier (*15*) [19], the signals from which are fed via a twisted cable to the recording unit for processing. The optical elements of the receiving system and preamplifier are located in the same metal housing.

The DLs operate in the pulse-periodic regime, when current pulses arrive at the lasers in series (temporal multiplexing). The injection currents for both DLs have an almost trapezoidal shape with steep fronts and a linear increase in the current in the gap, which provides approximately linear tuning of the DL wavelength. Temporal multiplexing allows the use of a single InGaAs photodetector to detect the radiation from both DLs propagating along the same path. This reduces the level of electrical noise, which is determined by the difference in photodetectors.

The radiation frequency of each DL is tuned within its spectral range (~3 cm^{-1}) for 20 ms, after which the generation of this DL stops for the same 20 ms during which the second DL operates. Thus, the minimum time for detecting experimental absorption spectra in the DLAS scheme is ~40 ms, not counting the transition time between the 'on' and 'off' regimes (~10 μs). In this scheme, the photodetector continuously detects signals of the radiation transmitted through the probe region, while the detection system allocates in time the signals corresponding to different wavelengths.

4. Results of experiments and their discussion

The performance characteristics of DLAS were tested by probing a homogeneous flame zone. These experiments, described in detail in [14], have demonstrated a good agreement between the temperatures of the homogeneous flame zone, independently determined by DLAS and CARS.

4.1. Temperature measurement

The effective flame temperature on the probe trace was measured in the transverse direction (x) and at different heights (z) from the plane of the burner slots ($z = 0$). To reduce signal fluctuations, the size of the focal spot was approximately 4 times smaller than the size of the photosensitive region of the receiver (2 mm). In this case, fluctuations in the spatial position of the beam passing through the hot region did not affect the signal intensity from the photodetector. The optical axis of the gradient collimator and the axis of the optical receiving system were pre-aligned so that the probe radiation transmitted through the flame was focused at the centre of photodetector *13*. The transverse distribution of the flame temperature was measured when the burner was moved along the x axis in the range from –12 to +12 mm in increments of 1 mm. In these experiments, the total length of the probe distance was 111 mm: 41 mm inside the flame and about 70 mm outside the flame (the sum of the lengths from the collimator end face to the flame and from the flame to photodetector *13*).

An example of the temperature distribution determined by DLAS in the x direction at a height of $z = 12$ mm is presented in Fig. 3. The same profile for a height of $z = 28$ mm is shown in Fig. 4. Both figures show the results obtained in the same flame using DLAS and CARS with N_2 molecules [13].

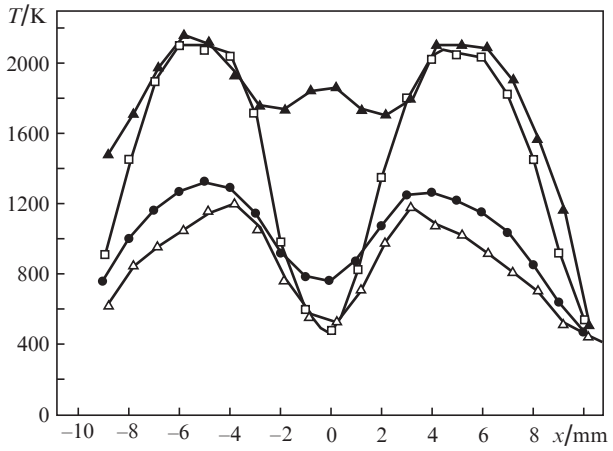

Figure 3. Spatial distributions of (□) local temperature determined by CARS [13], of (●) effective temperature T_{eff} determined by DLAS using the $1T$ algorithm, as well of (▲)T_{high} and (△) T_{low} calculated using the $2T$ algorithm along the x axis at $z = 12$ mm.

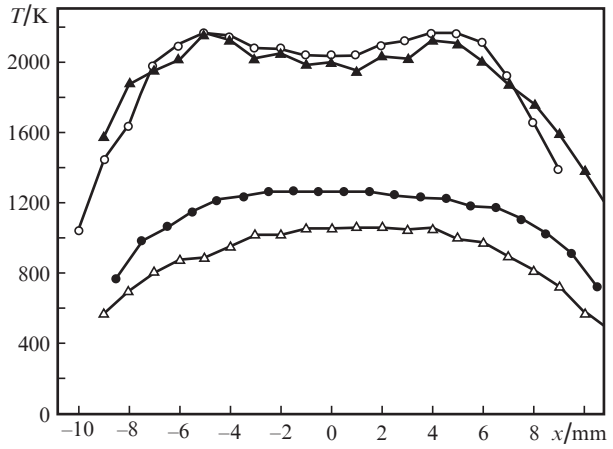

Figure 4. Spatial distributions of (○) local temperature determined by CARS [13], of (●) effective temperature T_{eff} determined by DLAS using the $1T$ algorithm, as well of (▲) T_{high} and (△) T_{low} calculated using the $2T$ algorithm along the x axis at $z = 28$ mm.

These results were obtained by processing the experimental DLAS absorption spectra using two algorithms: the $1T$ algorithm was used to estimate the effective temperature T_{eff}, while T_{low} and T_{high} were estimated using the $2T$ algorithm [see (2)]. In both cases, the NLS method was used to fit experimental spectra to theoretical ones.

4.2. Discussion of the results

To explain the results of the temperature estimation, it is necessary to understand the burner flame structure. For a flame with preliminary mixing of the fuel and oxidiser flows, the temperature profiles along the x axis at various heights were

experimentally studied in detail in [13]. The burner used in our experiments did not have additional protective air flows at the ends of the slits, which prevented combustion at the flame end faces [20, 21]. This led to the mixture combustion at both end faces in planes perpendicular to the main flame. As a result, transition zones with significant temperature gradients along the y axis were formed on both sides of the flame.

The results in Fig. 3 indicate that the proposed $2T$ algorithm works well enough for those flame cross sections in which zones with either high or low temperature prevail. Hot zones are located at $x \approx \pm 5$ mm and their temperatures are $\sim$2200 K; the cold zones are located in the middle of the flow mixing zone at $x \approx 0$ and their temperatures are $\sim$500 K. For these zones, the results obtained using the $2T$ algorithm are in good agreement with the results of local temperature measurements using CARS for the same flame sections. This is clearly seen in Fig. 3, which displays temperature distributions along the x axis at a height of 12 mm. These distributions are rather inhomogeneous; they have two peaks and a pronounced minimum. It can be seen that the temperatures at the two maxima determined by DLAS using the $2T$ processing algorithm are in good agreement with the local temperatures determined by CARS. The same good agreement is observed for minimum temperatures in the $x \approx 0$ region. We should stress again that the proposed $2T$ algorithm enables a good estimation of the temperature of those flame layers in which either a hot or a cold zone prevails.

Very interesting are the distributions at this height in the central part of the flame (-1 mm $< x <$ 1 mm). It should be noted that there is a significant difference between the temperature determined by CARS and the effective temperature T_{eff} determined by DLAS with the $1T$ processing algorithm. From our viewpoint, this difference is due to the hot flame layers located at the end faces of the slits in the direction perpendicular to the main flame (see Section 3.1). The structure of this section of flame at a height of 12 mm consists of a relatively cold section extended in the y direction and narrow hot layers at the end faces of the main flame [17], which make a significant contribution to the formation of the experimental absorption spectrum during trace probing by DLAS. As already noted, for this part of the flame, the estimation of T_{low} by DLAS using the $2T$ algorithm gives good agreement with the CARS results; however, when evaluating T_{eff} using the $1T$ algorithm, the temperature values turn out significantly overestimated due to the presence of additional end-face layers on the trace.

A very good agreement between the results of the two methods is also observed when determining the temperature distribution in the x direction at a height of 28 mm from the plane of slits (Fig. 4). At this height, the flame temperature profile is aligned, which is confirmed by local temperature measurements using CARS [13]. It can be seen that in the range of -6 mm $< x <$ 6 mm, the temperature determined by DLAS using the $2T$ algorithm coincides with the CARS results and is also virtually constant with a slight (50–100 K) increase towards the outer flame layers.

Note that in work [12] the spatial inhomogeneity of the test zone was experimentally simulated in the simplest way. i.e. using two cells of the same length with different temperatures of water vapour in them. The temperature distribution along the probe trace of the beam path was actually step-wise. This experimental model exactly matched the model of the proposed algorithm. It is not surprising that the results of determining two temperatures when using an adequate fitting algorithm turned out to be correct [12]. More interesting was the verification of the proposed $2T$ algorithm in fitting the absorption spectrum of laser radiation transmitted through a spatially inhomogeneous hot zone with an arbitrary temperature gradient. In this case, the two-temperature algorithm does not match the object structure. Nevertheless, the results of the study show that the proposed algorithm allows us to estimate the maximum and minimum temperatures of the inhomogeneous zone with sufficient accuracy. It should be noted that it is the maximum temperature of the combustion zone that is of greatest interest in the development of new engine designs.

5. Conclusions

A new approach is proposed for determining the maximum temperature in a spatially inhomogeneous hot zone by the trace DLAS method. The algorithm for processing the experimental absorption spectra of such an object, proposed in [12], was tested for an inhomogeneous object, i.e. the flame of a Wolfhard – Parker slot burner. The flame of such a burner is an example of a stationary, spatially inhomogeneous hot object. The proposed algorithm is based on fitting experimental spectra to a sum of single-temperature theoretical spectra. In the process of fitting, the summand coefficients are also the fitting parameters along with the temperature. In a DLAS spectrometer design, we used two distributed feedback DLs generating in the regions of 7185 and 7444 cm^{-1}. The radiation from both lasers was mixed in a multiplexer into a single beam that was directed into the flame. Various flame sections at various heights were probed. The results of measurements using DLAS were compared with the published results on diagnostics of such a flame using CARS [13].

At a height of 12 mm from the plane of the slits, the maximum and minimum temperatures along the probe trace, determined by DLAS using a new algorithm for processing experimental absorption spectra, are in good agreement with the CARS data. In these regions, the flame consists predominantly of either hot or cold zones.

A good agreement between the results of measurements by CARS and DLAS is observed for homogeneous flame sections at a height of 28 mm.

The proposed algorithm for fitting experimental spectra makes it possible to estimate with acceptable accuracy the maximum temperature of a spatially inhomogeneous hot zone; however, it does not allow determination of the temperature distribution profile in such an object.

Let us briefly discuss the main methodological differences between DLAS and CARS. They consist in the fact that DLAS allows one to estimate the temperature along the beam path in a single measurement, while CARS gives a temperature estimate within the local zone of intersection of laser beams with dimensions of the order of several millimetres. Thus, an estimation of the total volume of the test zone requires numerous measurements with a displacement of the beam intersection region within the object. Another important difference between CARS and DLAS is that the CARS diagnostics is virtually impossible in a small closed volume of combustion chambers, since obtaining an intense anti-Stokes coherent signal requires the intersection of laser beams at certain angles.

Acknowledgements. The authors express their gratitude to V.D. Kobtsev (Central Institute of Aviation Motors) for his assistance in conducting experiments with a burner.

References

1. Allen M.G. *Meas. Sci. Technol.*, **9**, 545 (1998).
2. Lackner M. *Rev. Chem. Eng.*, **23**, 65 (2007).
3. Schulz C., Dreizle A., Ebert V., Wolfrum J., in *Springer Handbook of Experimental Fluid Mechanics* (Berlin, Heidelberg: Springer, 2007) pp 1241–1315.
4. Bolshov M.A., Kuritsyn Yu.A., Romanovskii Yu.V. *Spectrochim. Acta Part B: At. Spectrosc.*, **106**, 45 (2015).
5. Goldenstein C.S., Spearrin R.M., Jeffries J.B., Hanson R.K. *Progr. Energy Combust. Sci.*, **60**, 132 (2017).
6. Liu C., Xu L. *Appl. Spectrosc. Rev.*; doi:10.1080/05704928.2018.1448854 (2018).
7. Gordon I.E., Rothman L.S., Hill C., Kochanov R.V., et al. *J. Quantum Spectrosc. Radiat. Transf.*, **203**, 3 (2017).
8. Rothman L.S., Gordon I.E., Barber R.J., Dothe H., et al. *J. Quantum. Spectrosc. Radiat. Transf.*, **111**, 2139 (2010).
9. Ma L., Li X., Sanders S.T., Caswell A.W., Roy S., Plemmons D.H., Gord J.R. *Opt. Express*, **21**, 1152 (2013).
10. Cai W., Kaminski C.F. *Progr. Energy Combust. Sci.*, **59**, 1 (2017).
11. Liu C., Cao Z., Lin Y., Xu L., McCann H. *IEEE Trans. Instrum. Meas.*, **67**, 1338 (2018).
12. Liger V.V., Mironenko V.R., Kuritsyn Yu.A., Bolshov M.A. *Sensors*, **18**, 1608 (2018).
13. Datta A., Beyrau F., Seeger T., Leipertz A. *Combust. Sci. Technol.*, **176**, 1965 (2004).
14. Liger V.V., Mironenko V.R., Kuritsyn Yu.A., Bolshov M.A. *Quantum Electron.*, **48**, 1055 (2018) [*Kvantovaya Elektron.*, **48**, 1055 (2018)].
15. Wolfhard H.G., Parker W.G. *Proc. Phys. Soc. Sect. A*, **65**, 2 (1952).
16. Smyth K.C., Miller J.H., Dorfman R.C., Mallard W.G., Santoro R.J. *Combust. Flame*, **62**, 157 (1985).
17. Liger V.V., Kuritsyn Yu.A., Mironenko V.R., Bolshov M.A., Ponurovskii Ya.Ya., Kolesnikov O.M. *High. Temp.*, **56**, 98 (2018) [*Teplofiz. Vys. Temp.*, **56**, 92 (2018)].
18. Sacher Lasertechnik; http://www.sacher-laser.com/home/laser-diodes/distributed_feedback_laser/dfb/single_mode.html.
19. Liger V.V. *Instrum. Exp. Tech.*, **60**, 453 (2017) [*Prib. Tekh. Eksp.*, (3), 148 (2017)].
20. Miller J.H., Elreedy S., Ahvazi B., Woldu F., Hassanzadeh P. *Appl. Opt.*, **32**, 6082 (1993).
21. Wagner S., Fisher B.T., Fleming J.W., Ebert V. *Proc. Combust. Inst.*, **32**, 839 (2009).